Evaluation of Critical Operating Conditions for a Semi-batch Reactor by Complementary Use of Sensitivity and Divergence Criteria

G. Maria* **and D.-N. Stefan**
Department of Chemical Engineering,
University Politehnica of Bucharest, Romania

Original scientific paper
Received: April 26, 2010
Accepted: September 26, 2010

This paper presents a comparison of several effective methods of deriving the critical feeding conditions for the case of a semi-batch catalytic reactor used for the acetoacetylation of pyrrole with diketene in homogeneous liquid phase. The reaction is known to be of high risk due to the very exothermic (polymerisation) side-reactions involving reactive diketene. In order to perform the sensitivity analysis, both the Morbidelli-Varma sensitivity criterion and *div*-methods were used, the latter of which are based on the system's Jacobian and Green's function matrix analysis. The combined application of such criteria allows the optimal and safe setting of the reactor's nominal operating conditions. Extended sensitivity analysis reveals possible QFS (quick onset, fair conversion and smooth temperature profile) regions, under severe operating conditions characterized by fast enough main reaction that prevents the co-reactant accumulation, and leads to a quasi-insensitive semi-batch reactor behaviour.

Key words:
Critical conditions, semi-batch reactor, sensitivity, divergence, pyrrole, diketene

Introduction

Setting the chemical reactor's technological constraints and runaway boundaries of the operating conditions are important for both risk assessment and over-design avoidance. Whenever the reactor's economic performance is the most important factor, the frequent solution entails a risky operation very close to the safety limits, where the runaway can occur due to either a malfunction in the cooling system or highly exothermic side reactions (even when implementing an advanced control system).

Knowledge of the safety limits and their confidence region is important not only for optimally setting the nominal operating conditions of the reactor, but also for implementing a real-time on-line algorithmic sensor to detect system instability in the proximity of critical conditions (early warning detection), thus preventing the process runaway. The process analysis must also consider the variability of the process conditions and sometimes the uncertainty in model parameters in order to increase the confidence of the predicted critical conditions.

The present study is focused on analysing combined methods for detecting the critical conditions in a semi-batch reactor (SBR). Such reactors are more and more preferred due to the possibility of controlling an exothermic chemical reaction and reactor temperature by the policy of adding one of the reactants to the other components, which have already been fully loaded to the reactor. As a consequence, the probability of co-reactant's accumulation is drastically reduced; moreover, in case of abnormal behaviour of the reactor, simply reducing the dosing rate can stop the process. On the other hand, it is the current trend to move production of a lot of chemicals from the stable continuous plants to multi-product (semi-)batch reactors, as they are more flexible and easily adaptable to market requirements. A certain optimal feeding policy can ensure production maximization, even if frequent perturbations in the operating parameters, raw-materials and recycling conditions, catalyst characteristics and presence of impurities from previous batches, all require periodical model, feeding policy, and safety limits updates.

One simple but approximate way to determine the operation safety limits is to use explicit methods, i.e. simple relationships derived from experimental observations on the reactor's thermal sensitivity, or from simplifying more complicated model-based criteria. Simple engineering numbers (such as Damköhler-*Da*, Stanton-*St*, or Lewis), or safety indices may give an approximate idea on the runaway limits and many times replace the systematic model-based safety analysis of the process.[1–6] Even if quickly applicable, such calculations are not sufficiently accurate for an advanced optimization of the process or for implementing an on-line instability detector.

*Corresponding author; Mail address: P.O. 35–107 Bucharest, Romania; Email: gmaria99m@hotmail.com

Model based evaluations of critical operating conditions, even if more laborious and requiring a steady effort to up-date the model parameters to process changes, offer a quite accurate prediction of the safety region and are generally applicable to every reactor type. According to Adrover *et al.*,[7] such criteria used in characterization and diagnosis of reactor runaway and explosion can be classified into four categories: geometry-based criteria, parametric sensitivity-based criteria, divergence-based criteria, and stretching based criteria.

Geometry-based methods (GM) interpret the shape of the temperature or heat-release rate profile over the reaction (contact) time. Critical conditions correspond to an accelerated temperature increase, i.e. to an inflexion point before the curve maximum in a temperature – time plot $T(t)$.

Sensitivity-based methods (PSA) detect unsafe conditions as those characterized by high parametric sensitivities of state variables x_i with respect to operating parameters ϕ_j, i.e. $s(x_i;\phi_j) = \partial x_i/\partial \phi_j$ (in absolute terms), that is, where "the reactor performance becomes unreliable and changes sharply with small variations in parameters".[2] Local sensitivity analysis (developed for every state variable and parameter), or global sensitivity analysis (extended over the whole reactor and operation time, by accounting for concomitant variations of several input/process parameters) eventually lead to global runaway conditions of the reactor.[4–6]

Divergence (div-)based criteria identify any instability along the system/process evolution and detect any incipient divergence from a reference (nominal condition) state-variable trajectory over the reaction time $x_i(t)$. Any increased sensitivity of the system stability in the proximity of runaway boundaries in the parametric space is detected from analysing the eigenvalues of the process model Jacobian ($\boldsymbol{J}$) and Green's ($\boldsymbol{G}$) function matrices, evaluated over the reaction time.[8,9] More elaborated versions use more sophisticated *div*-indices to characterize the expansion of volume elements in phase-space (having state variables as coordinates), e.g. Lyapunov exponents based on the analysis of the time-dependent $\boldsymbol{J}^T\boldsymbol{J}$ matrix.[10,11]

Stretching based analysis (SBA), recently introduced by Adrover *et al.*,[7] combines sensitivity and *div*-methods by investigating the dynamics of the tangent components to the state-variable trajectory. Critical conditions are associated with the system's dynamics acceleration ('stretching rates' of the tangent vectors), corresponding to a sharp peak of the normalized stretching rate due to the accelerate divergence from the nominal trajectory.

Each critical condition method presents advantages and limitations related to precision, real-time application, involved computational effort, and local applicability. Several classification criteria can be defined to assess the generality of each method,[7] such as: objectivity (validity independent on particular choice of the system or operating conditions of a checked process); generality (general validity, independent on the process or reactor type); real-time applicability (as on-line algorithmic sensor to detect instabilities and runaway conditions); locality (the use of local quantities or model linearizations). According to such a classification, all mentioned method types are objective, all methods are generally applicable excepting GM, all methods can be on-line used for real-time runaway detection excepting PSA, and only PSA and SBA are global methods following the current $\boldsymbol{x}(t)$ vector evolution.

The combined use of several methods is recommended to increase the prediction precision but also the applicability area. Because geometrical methods tend to overestimate the stability region, or sometimes they are too conservative thus producing unnecessary warnings,[2,8,11] PSA methods are preferred, by offering precise predictions of runaway boundaries due to the possibility of choosing between process parameters when calculating the sensitivity functions. However, PSA precision limitations in low sensitive operating regions,[5,8,12] and impossibility of an on-line use require supplementary checks by means of *div*-methods. Even if precision problems are inherent due to model linearization in the proximity of high sensitive operating regions, the possibility to on-line diagnose the process for an early stage runaway compensate the *div*-method drawbacks.[10,31]

However, SBR may pose serious operating problems when highly exothermic reactions are conducted, especially when the primary reaction is slow *vs.* addition time, while secondary reactions quickly occur at any incidental increase of reaction temperature. Runaway occurs when the rate of heat generation becomes faster than the rate of heat removal by the design cooling system. In the homogeneous reaction case, the accumulation of the co-reactant at low temperatures, leads to an exponential rise in the reaction rates for any temperature increase, which in turn will generate large reaction heat fluxes overstepping the heat removal possibilities of the cooling system. The situation is worsened when secondary exothermic chain / polymerisation reactions are inducted by high temperatures, leading to a quick increase in temperature or pressure with eventually the same effect.[1–3] Conditions of runaway are also derived for heterogeneous liquid-liquid SBR.[13] Such safety considerations when

conducting highly exothermic reactions encourage the reactor overdesign (with additional costs), and operation with a conservative, under-optimal operating strategy to prevent accumulation of the co-reactant in the reactor.[14–16] Therefore, separate supervision of each SBR, periodical / on-line updates of the safety margins for the operating variables based on a process model, and a combined application of diagnosis / runaway criteria become necessary.

The sensitivity based analysis can be completed with detection of the so-called "Quick onset, Fair conversion and Smooth temperature profile" (QFS) super-critical operating regions, characterized by a high level but quite 'flat' temperature-over-time-profile, and small sensitivities of state variable *vs.* operating conditions. Such regions can be of economic interest and should be accounted for determining the optimal operating policy of the industrial SBR. Classification of the operating regions in non-ignition, marginal ignition, runaway, and QFS is not easy, and depends on the accumulation of the co-reactant, temperature regime, and reaction characteristics.[32,33] Steensma and Westerterp[32] indicated some criteria to characterise the operating region, and pointed-out that "the obtaining of a smooth, stable, and realistic target temperature is more important than a sharp limitation of the accumulated mass, or a limitation of the maximum conversion rate".

The present paper aims at evaluating, comparing, and investigating coupling possibilities of some sensitivity and *div*-criteria to offer precise predictions of critical conditions and their confidence intervals for a SBR together with the possibility of an early detection of the runaway proximity. Such a combination allows a more precise SBR optimization and implementation of an on-line algorithmic sensor to detect any system instability. The examined SBR is the bench-scale jacketed reactor for the acetoacetylation of pyrrole with diketene to PAA (2-acetoacetyl pyrrole) in homogeneous liquid phase, used by Ruppen *et al.*[17] to identify the optimal isothermal feeding policies that maintain the reactor within technological limits and lead to an acceptable PAA product yield. Recently, Maria *et al.*[6] approached this high-risk SBR case study and have used a non-isothermal reactor model to derive the critical conditions by means of the generalized sensitivity criterion of Morbidelli-Varma (MV).[2] The present study extends the analysis by accounting for several runaway criteria completed with identification of possible QFS operating regions of economic interest.

Sensitivity and divergence criteria of critical operating conditions

The current study is focused on evaluating the critical conditions for a semi-batch reactor by using the MV sensitivity criterion, and three *div*-criteria (denoted with *div*-J, *div*-SZ, and *div*-LY, see below). These runaway criteria are chosen to combine the evaluation precision/robustness with the sensitivity in detecting any system small instability of chemical process referring to a nominal evolution.

The generalized sensitivity criterion MV. This criterion associates the critical operating conditions with the maximum of sensitivity of the hot spot $(T_{\max} - T_0)$ in the reactor, evaluated over the reaction time, in respect to a certain operating parameter ϕ_j. In other words, critical value of a parameter $\phi_{j,c}$ corresponds to:

MV criterion:

$$\begin{gathered}\phi_{j,c} = \arg\left(\max_{\phi_j}\left|s(T_{\max};\phi_j)\right|\right),\\ \text{or } \phi_{j,c} = \arg\left(\max_{\phi_j}\left|S(T_{\max};\phi_j)\right|\right),\\ S(T_{\max};\phi_j) = (\phi_j^*/T_{\max}^*)\cdot\\ \cdot s(T_{\max};\phi_j) = (\phi_j^*/T_{\max}^*)(\partial T_{\max}/\partial\phi_j),\end{gathered} \tag{1}$$

[where: $S(T_{\max}/\phi_j)_t$ – relative sensitivity function of $T_{\max}$ *vs.* parameter ϕ_j; '*' – nominal operating conditions (set point) in the parameter space; t – reaction time].

According to the MV criterion, critical conditions induce a sharp peak of the normalized sensitivity $S(T_{\max};\phi_j)$ evaluated over the reaction time and over a wide range of ϕ_j. The robustness and effectiveness of the MV-criteria derives from the general validity, irrespectively to the complex reaction pathway, reactor configuration, or the considered operating parameter ϕ_j (e.g. T_0, $c_{j,0}$, Q_{inlet}, $c_{j,\text{inlet}}$, T_a, B, Da, St, …, or a combination of them, see the notation list for symbol definitions). The sensitivity functions $s(x_i;\phi_j)$ of the state variables x_i (including the reactor temperature) can be evaluated by using the so-called 'sensitivity equation' solved simultaneously with the reactor model:[2]

$$\begin{gathered}\frac{\mathrm{d}s(\boldsymbol{x};\phi_j)}{\mathrm{d}t} = \frac{\partial \boldsymbol{g}}{\partial \boldsymbol{x}}s(\boldsymbol{x};\phi_j) + \frac{\partial \boldsymbol{g}}{\partial \phi_j};\\ s(x;\phi_j)\big|_{t=0} = \delta(\phi_j - x_0),\\ \mathrm{d}\boldsymbol{x}/\mathrm{d}t = \boldsymbol{g}(\boldsymbol{x},\boldsymbol{\phi},t),\ \ \boldsymbol{x}|_{t=0} = \boldsymbol{x}_0,\end{gathered} \tag{2}$$

(where the Kronecker delta function $\delta(\phi_j - x_0)$ takes the value 0 for $\phi_j \neq x_0$, or the value 1 for $\phi_j = x_0$). Evaluation of derivatives in (2) can be precisely performed by using the analytical derivation or, being less laborious, by means of numerical derivation. A worthy alternative, also used in the present study, is the application of the numerical finite difference method, which implements a certain differentiation scheme (of various precision and complexity) to estimate the derivatives of $s(x_i;\phi_j)_t$ at various reaction times.[18] However, the method becomes computationally costly when approaching the runaway boundaries because precise evaluation of the state's high sensitivities requires small discretization steps in the parameter space.[6] Also, the runaway boundary predictions become approximate for very severe operating conditions where super-criticality can induce a quasi-insensitivity of the temperature maximum to operating conditions.[12]

Div-J criterion. The divergence criteria are derived from the dynamical systems theory, from characterization of chaotic attractors in dynamical systems.[7] In the *div*-J variant of Hegdes and Rabitz,[19] one considers a reference solution $x^*(t)$, usually known as set point or nominal conditions, and one investigates the effect of any perturbation in the initial conditions $x_{i,0}$ or parameter ϕ_i by inspecting the eigenvalues of the system Jacobian $\lambda_i(\boldsymbol{J})$. These eigenvalues prescribe how perturbations behave for small time intervals near every considered moment. When the real part of only one eigenvalue becomes positive at a certain time, this perturbation induces system instability and divergence of the state-variable time-trajectory from the reference solution. In the risk assessment, such instability is associated with the occurrence of critical conditions determining process runaway. Zaldivar *et al.*[9] introduced an early detection of loss of stability as those corresponding to occurrence of the Jacobian trace positiveness, i.e. for $Trace(\boldsymbol{J}) = \sum_i \lambda_i > 0$. Starting from the Vajda and Rabitz[8] observation that critical conditions correspond to the positive extreme point of $\mathrm{Re}(\lambda(\boldsymbol{J}))$ evaluated at the temperature peak, in the present work the critical value of a checked parameter $\phi_{j,c}$ is estimated based on:

div-J criterion:

$$\phi_{j,c} = \min(\phi_j),$$

$$\text{for which } \max_i(\max_t(\mathrm{Re}(\lambda_i(\boldsymbol{J}(\phi_j))))) > 0,$$

where:

$$\boldsymbol{J} = (\partial \boldsymbol{g}/\partial \boldsymbol{x})_t;\ \mathrm{d}\boldsymbol{x}/\mathrm{d}t = \boldsymbol{g}(\boldsymbol{x},\boldsymbol{\phi},t),\ \boldsymbol{x}|_{t=0} = \boldsymbol{x}_0, \quad (3)$$

(when more severe conditions correspond to smaller ϕ_j, then $\max(\phi_j)$ must be taken in the criterion, e.g. for $\phi_j = Da$, or $\phi_j = Da/St$). The evaluation rule starts by computing $\mathrm{Re}(\lambda_i(\boldsymbol{J}))$ values at various reaction times for a certain small ϕ_j value, and keeping the other parameters at nominal values. If the condition (3) is not satisfied, the parameter ϕ_j is increased with a small increment (to ensure a reasonable evaluation precision) and the procedure is repeated until the critical value is identified. Evaluation of the ***J***-matrix elements is made analytically with high precision, for instance by applying commercial software for symbolic calculation, such as Maple package in the present work.[20]

Div-SZ criterion. A convenient *div*-criterion alternative detects the possible loss of system stability by investigating the expansion of volume elements $V(t)$ in phase-space having state variables as coordinates (the so-called Strozzi-Zaldivar SZ-criterion).[10,11] The ellipsoidal volume having the point $\boldsymbol{x}(t)$ in the centre is calculated at every moment t, by considering the volume expansion from an initial state $\boldsymbol{x}_0$ due to variations $\delta\boldsymbol{x}$ of the state-vector components. Such volume elements' expansion / contraction corresponds to the solution $\boldsymbol{x}(t)$ divergence / convergence toward the reference trajectory. Checking evolution of ellipsoidal volume semi-axes, through the so-called Lyapunov exponents $\tilde{\lambda}_i$, better monitors the system evolution after a parametric perturbation:

$$\tilde{\lambda}_i(t) = \frac{1}{t}\log_2\frac{|q_i(t)|}{|q_i(0)|} = \log_2\sqrt{\lambda_i(\boldsymbol{J}^T\boldsymbol{J})}, \quad i = 1,\ldots,\mathrm{size}(\boldsymbol{x}). \quad (4)$$

(where: $\boldsymbol{q}$ – orthogonalized vectors of $\boldsymbol{x}$; size ($\boldsymbol{x}$) – dimension of the vector $\boldsymbol{x}$). If the volume semi-axis expands, the corresponding Lyapunov exponent will be positive. Consequently, for a higher dimension of state vector, the critical conditions correspond to the extreme of the sensitivity function of the sum of Lyapunov exponents:

$$\phi_{j,c} = \arg(\max_{\phi_j}(\max_t(s(V(t);\phi_j)))); \quad V(t) = 2^{\sum_i \tilde{\lambda}_i(t)}. \quad (5)$$

An equivalent form of the Lyapunov exponent criterion was proposed in this paper, by associating critical condition $\phi_{j,c}$ to a sharp change of slope in the plot of positive maximum of Lyapunov exponents *vs.* ϕ_j, that is:

div-SZ criterion:

$$\phi_{j,c} = \min(\phi_j),$$

$$\text{for which } \max S(L_{\max};\phi_j) > \sigma_j,$$

where:

$$L_{\max} = \max_i\left(\max_t\left(\sqrt{\lambda_i(\boldsymbol{J}^T\boldsymbol{J})}\right)\right),$$

$$S(L_{\max};\phi_j) = \partial \ln(L_{\max})/\partial \ln(\phi_j), \quad (6)$$

$$\boldsymbol{J}(\phi_j) = (\partial \boldsymbol{g}/\partial \boldsymbol{x})_t;\ \mathrm{d}\boldsymbol{x}/\mathrm{d}t = \boldsymbol{g}(\boldsymbol{x},\boldsymbol{\phi},t),\ \boldsymbol{x}|_{t=0} = \boldsymbol{x}_0.$$

The relative tolerance σ_j of sensitivity of the SZ-criterion with respect to the *j*-th parameter can be chosen in relation with the known standard deviation (in relative terms) of the parameter value due to (assumed) normal fluctuations,[21] but other a-priori values can also be adopted.

Div-LY criterion. When the number of reactions is much larger than that of the considered species in the process model, an alternative runaway diagnostic method is the *div*-LY criteria based on the analysis of the eigenvalues of the Green's function matrix $\boldsymbol{G}$.[2] The Green's functions $G_{ij} = \partial x_i(t)/\partial x_{i0}$ are in fact the sensitivities of the state variables $\boldsymbol{x}$ to the initial conditions, being evaluated from the model Jacobian, by using the differential equation integrated simultaneously with the reactor model:[19]

$$\begin{gathered}\mathrm{d}\boldsymbol{G}/\mathrm{d}t = \boldsymbol{J}(\boldsymbol{x}(t))\boldsymbol{G},\quad \boldsymbol{G}(0) = \boldsymbol{1},\quad \boldsymbol{J} = \partial \boldsymbol{g}/\partial \boldsymbol{x},\\ \mathrm{d}\boldsymbol{x}/\mathrm{d}t = \boldsymbol{g}(\boldsymbol{x},\boldsymbol{\phi},t),\quad \boldsymbol{x}(0) = \boldsymbol{x}_0.\end{gathered} \quad (7)$$

At critical conditions, at least one eigenvalue of $\boldsymbol{G}$ [denoted as $\lambda_j(\boldsymbol{G})$] diverges from zero or, equivalently, the asymptotic Lyapunov stability numbers $\alpha_i(t)$ diverge. In the present study, an equivalent formulation is proposed, by associating the critical condition $\phi_{j,c}$ to a sharp change of slope in the plot of positive maximum of Lyapunov numbers *vs.* ϕ_j, which is equivalent to:

div-LY criterion:

$$\phi_{j,c} = \min(\phi_j),$$

$$\text{for which } \arg(\max_{\phi_j}(S(LY_{\max};\phi_j))) > \sigma_j,$$

where:

$$\begin{gathered}LY_{\max} = \max_i(\max_t(\alpha_i(t))),\\ S(LY_{\max};\phi_j) = \partial \ln(LY_{\max})/\partial \ln(\phi_j),\\ \alpha_j(t) = \ln|\lambda_j(\boldsymbol{G})|/(t - t_0).\end{gathered} \quad (8)$$

Finally, it is worth mentioning that regardless of the method used, the safety analysis of the SBR continues to be of high interest due to the frequent problems associated with the variability in operating conditions inducing non-linear behaviours of complex processes and the requirement to up-date/optimise the reactor operation when the raw-material/catalyst properties change. On the other hand, the chosen nominal operating point tries to limit the hot spot during the batch, and thus avoid an excessive sensitivity to variations in the process parameters.

This is why other safety criteria continue to be developed by combining the sensitivity and loss of local stability criteria, by analysing the characteristics of the system Jacobian, Green's function matrix, Lyapunov numbers, tangent components to the state-variable trajectory, or other combinations of them during the process evolution.[7,22–24]

QFS region detection. Another interesting aspect to be investigated is the detection of the so-called "Quick onset, Fair conversion and Smooth temperature profile" (QFS) operating region in the parametric space. In QFS regions, usually located in the super-critical / high severity operating area, the SBR temperature displays a quite 'flat' time-profile, even if at a higher level. The QFS region actually belongs to the ignition behaviour, and is explained by the fact that, under high severity conditions the reactions occur quasi-instantaneously, and accumulation of the co-reactant is no longer possible. Thus, the temperature profile becomes quasi-flat, SBR displays a low thermal sensitivity, and its operation in such a region makes sense if other technological constraints are not active. Moreover, investigation of the QFS location at severe conditions becomes important when establishing the optimal operating "set-point" of the reactor from both economic and safety perspectives.

For a single reaction case, Alos *et al.*[12,30] proposed to determine the boundary of the QFS region based on evaluation of the time to reach the maximum temperature in the reactor (denoted here with $t_{\max}$). Starting from the observation that $t_{\max} - \phi$ curve passes through a minimum in a region where it is quite insensitive to ϕ (irrespectively to the ϕ parameter choice), the condition for starting the QFS region becomes:[12,24]

$$\begin{gathered}\phi_{QFS} = \arg(s(t_{\max};\phi) = 0),\\ \text{(i.e. } t_{\max}(\phi) \text{ presents a minimum).}\end{gathered} \quad (9)$$

By repeating this rule, and every time determining ϕ_{QFS} for different values of a certain operating parameter (e.g. φ), the QFS boundary curve

$\phi_{QFS}(\varphi)$ results in the parametric plane $\phi - \varphi$. For a single reaction case, the limit of the QFS region usually corresponds to SBR running conditions that are even more severe than the runaway limit. Eventually, the quasi-insensitive QFS region has to be confirmed by the quasi-flatness of the temperature evolution over the batch time, and its maximum occurrence later than the minimal t_{max} value. The validity of the QFS-criterion was experimentally confirmed for simple reaction cases.[12] Since the MV-sensitivity criterion cannot distinguish between the runaway and the QFS regions because in both cases the reaction is ignited, the use of the QFS-criterion in locating alternative operating region of economic interest is well supported. This rule is similar[12] to the so-called "target temperature criterion" of Steensma and Westerterp[32,33] which uses two dimensionless numbers (reactivity and exothermicity) together with a definition of the target temperature of the SBR to frame each running point in the non-ignition, marginal ignition, runaway, or QFS region.

Acetoacetylation of pyrrole – process characteristics

The acetoacetylation of pyrrole (P) with diketene (D) is conducted in homogeneous liquid phase (toluene), at around 50 °C and normal pressure, using pyridine as catalyst, for producing pyrrole derivates such as PAA used in the drug industry. The process is of high thermal risk due to the tendency of the very reactive diketene to polymerise at temperatures higher than 60–70 °C, or in the presence of impurities that can initiate highly exothermic side reactions difficult to be controlled.[25] The complex process kinetics have been investigated by Ruppen *et al.*[17] in a bench-scale isothermal SBR operated at 50 °C using a high excess of toluene as solvent.

The proposed kinetic model from Table 1 accounts for only four exothermic reactions: (a) the synthesis of PAA (P + D → PAA) is accompanied by several side-reactions of diketene, leading to its dimmer (b)(2D → DHA; DHA = dehydroacetic acid), and oligomers (c)(nD → D_n), or to a by-product denoted by G (d)(PAA + D → G; the intermediate reaction of diketene with DHA has been neglected from the model). Because the co-reactant diketene presents extreme reactivity and hazardous properties, the temperature regime must be strictly controlled and the diketene and DHA concentrations in the reactor kept lower than certain critical thresholds (empirically determined, see Table 1).[17,26] The rate constants have been evaluated by Ruppen *et al.*[17] at 50 °C and [PAA] > 0.1 mol L^{-1}.

Maria *et al.*[6] completed the model by including the Arrhenius dependence of the main rate constants, and by adopting an activation energy of $E/R = 10242$ K for all reactions of diketene, by analogy with the diketene derivate polymerisation, and with the initiation energy of olefin polymerization. The resulting Arrhenius constants (A_i, E_i) are displayed in Table 1. All reactions are moderately exothermic, except for the diketene oligomerization of standard heat around –1423 kJ mol^{-1}.

Based on these thermodynamic-kinetic data, Maria *et al.*[6] performed a quick assessment of the reaction hazard, which indicates reactions (*a*) and (*c*) as being dangerous even under the nominal operating conditions displayed in Table 1, presenting: $\Delta T_{ad} = 62$ K (reaction *a*) and $\Delta T_{ad} = 83$ K (reaction *c*), i.e. larger than the threshold 50 K; $B = 6$ (reaction *a*) and $B = 8.1$ (reaction *c*), i.e. larger than the threshold 5; $Da = 1.7$ (reaction *b*) and $Da = 4.2$ (reaction *c*), i.e. smaller than the threshold 50–100 (slow reactions).[1] Calculations have been made using the common relationships:[1]

$$\Delta T_{ad} = (-\Delta H)\, c_{j,0}/(\overline{\rho}\,\overline{c}_p), \quad B = \Delta T_{ad} E/(RT_0^2), \quad Da = (-\nu_j)(r_j \tau_D)/c_{j,0} \tag{10}$$

(where: ΔT_{ad} – adiabatic temperature rise; B – reaction violence index; Da – Damköhler number for the key reactant j; $c_{j,0}$ – initial concentration of key species; $\overline{\rho}$ – reacting mixture density; $\overline{c}_p$ – average specific heat; T_0 – initial/cooling agent temperature of the reaction; R – universal gas constant; $(-\nu_j)$ – stoichiometric coefficient of reactant j; τ_D – co-reactant adding time).

For a quick process simulation, a simple SBR model was adopted, corresponding to a perfectly mixed vessel, with no mass and heat transfer resistances in the liquid.[27] The solution of diketene in toluene is continuously added with a variable fed flow-rate $Q(t)$ over the continuously stirred pyrrole solution (including impurities) initially loaded to the jacketed reactor, and the reaction heat is continuously removed through the reactor wall. The mass and heat balance equations, presented in Table 1, explicitly account for the liquid volume and heat transfer area increase during the batch. The continuous catalyst dilution is accounted for when correcting the reaction rates, except for reaction (c) presumed to be promoted not by pyridine but by some impurities (of quasi-constant concentration). To speed-up the computational steps, the physical properties of the reaction mixture have been approximated to those of the toluene solvent, and a constant overall heat transfer coefficient has been evaluated (Table 1).

Table 1 – *Process and semi-batch reactor model, nominal operating conditions, and technological constraints. (Notations: D = diketene; P = pyrrole; PAA = 2-acetoacetyl pyrrole; DHA = dehydroacetic acid; Py = pyridine).*[6]

Process main reactions and reduced kinetic model (Footnote a):

$P + D \xrightarrow{k_a, Py} PAA$; $r_a = k_a c_P c_D$; $k_a = 3.1324 \cdot 10^{12} \exp(-10242.4/T)$, L mol^{-1} min^{-1};

$\Delta H_a = -132.69$ kJ mol^{-1}; $\Delta T_{ad} = 61.8$ K

$D + D \xrightarrow{k_b, Py} DHA$; $r_b = k_b c_D^2$; $k_b = 7.5651 \cdot 10^{12} \exp(-10242.4/T)$, L mol^{-1} min^{-1};

$\Delta H_b = -91.92$ kJ mol^{-1} ; $\Delta T_{ad} = 5.3$ K

$n D \xrightarrow{k_c} (D)_n$; $r_c = k_c c_D$; $k_c = 1.6549 \cdot 10^{12} \exp(-10242.4/T)$, min^{-1};

$\Delta H_c = -1426.12$ kJ mol^{-1} ; $\Delta T_{ad} = 83.0$ K

$PAA + D \xrightarrow{k_d Py} G$; $r_d = k_d c_{PAA} c_D$; $k_d = 1.7731 \cdot 10^{12} \exp(-10242.4/T)$, L mol^{-1} min^{-1};

$\Delta H_d = -132.69$ kJ mol^{-1}; $\Delta T_{ad} = 7.7$ K

Differential balance equations:

– species mass balance: $\frac{dc_D}{dt} = (-\tilde{r}_a - 2\tilde{r}_b - \tilde{r}_c - \tilde{r}_d) + (c_{D,in} - c_D)\frac{Q(t)}{V(t)}$; $\frac{dc_P}{dt} = -\tilde{r}_a - c_P \frac{Q(t)}{V(t)}$;

$\frac{dc_{PAA}}{dt} = (\tilde{r}_a - \tilde{r}_d) - c_{PAA} \frac{Q(t)}{V(t)}$; $\frac{dc_{DHA}}{dt} = \tilde{r}_b - c_{DHA} \frac{Q(t)}{V(t)}$; volume variation: $\frac{dV}{dt} = Q(t)$;

– reaction rate correction with the catalyst dilution: $\tilde{r}_j = r_j \frac{V_0}{V(t)}$; $j = a,b,d$

– heat balance: $\frac{dT}{dt} = \frac{Q(t)(T_{in} - T)}{V(t)} + \frac{\sum_j (-\Delta H_j)\tilde{r}_j V(t) - U A_r (T - T_a)}{\bar{\rho}\,\bar{c}_p V(t)}$, $j = a,b,c,d$

Observations: i) at $t = 0$, $c_j = c_{j,0}$, $T = T_0$; ii) r_C is not corrected with the catalyst dillution, the reaction displaying another mechanism (the stoichiometric coefficient was included in the rate constant)

Model hypotheses:

– semi-batch reactor model with perfect mixing and uniform concentration and temperature field

– cylindrical reactor of variable liquid volume and heat transfer area: $A_r = \frac{\pi d_r^2}{4} + \frac{4}{d_r} V(t)$

– overall heat transfer coefficient evaluated with criterial formula[27] (approximate value for nominal conditions is $U = 581$ W m^{-2} K^{-1})

– heat of solvent vaporisation in the reactor is neglected

– specific heat capacity and density of fed solution are the same with those of reactor content, $\bar{\rho}_{in}\bar{c}_{p,in} \approx \bar{\rho}\,\bar{c}_p$

Nominal operating conditions and range of variation

initial liquid volume (V_0, L):	1	initial [PAA] (mol L^{-1}):	0.08 ≤ 0.10 ≤ 0.20
reactor inner diameter (d_r, m):	0.1	initial [DHA] (mol L^{-1}):	0.01 ≤ 0.02 ≤ 0.04
stirrer speed (r min^{-1}):	640	fed D solution flow rate ($Q \cdot 100$, L min^{-1}):	0.05 ≤ 0.15 ≤ 0.20
liquid physical properties:	toluene solvent	batch time (t_f, min):	120 ≤ 145 ≤ 378
inlet [D] (mol L^{-1}):	4 ≤ 5.82 ≤ 6	initial temperature (θ_0, °C):	40 ≤ 50 ≤ 60
initial [P] (mol L^{-1}):	0.4 ≤ 0.72 ≤ 0.8	cooling agent temperature (θ_a, °C):	50
initial [D] (mol L^{-1}):	0.005 ≤ 0.09 ≤ 0.14	feeding solution (θ_{in}, °C):	50

Process constraint expression:	*Significance*
$c_{DHA,f} - 0.15 \le 0$, (mol L^{-1})	Prevent precipitation of DHA at room temperature (solubility at 50 °C is 0.20 mol L^{-1})[17]
$c_{D,f} - 0.025 \le 0$, (mol L^{-1})	Avoid high concentrations of toxic D in product;[17] empirical critical runaway condition.[26]
$\max(\theta(t)) - 70 \le 0$, ($\theta$, °C)	Prevent toluene solvent excessive vaporization, pressure increase, and dangerous exothermic side-reactions (Footnote b)

Footnotes:

(a) $\Delta T_{ad} = (-\Delta H)\, c_{j,0} / (\bar{\rho}\,\bar{c}_p)$.

(b) Empirically predicted by adding $2 \cdot \Delta T_c = 20$ K to the nominal temperature, where $\Delta T_c = RT_0^2 / E$ correspond to the critical conditions of Semenov for zero-order reactions.[1]

Simulations of the reactor dynamics reveal a high thermal sensitivity due to side-reaction thermal effect.[6] Starting from feed levels approximately higher than Q = 0.070–0.0080 L min^{-1}, the temperature $T(t)$ profile not only exhibits values higher than the critical threshold of 70 °C (technological constraint of Table 1), but tends to become oscillatory. Higher feed flow rates produce amplification of oscillations, toluene vaporization, a dangerous pressure increase, and eventually the reactor runaway. Such an effect can be explained by the slow secondary reactions (b-c) (diketene exothermic oligomerization), which become dangerous when the co-reactant D is accumulating at low temperatures. For small feeding Q-levels the main reaction consumes the co-reactant, and the side-reactions are negligible. Contrariwise, at high input Q-levels the slow side-reactions lead to the co-reactant D accumulation, which will generate more energy increasing the reactor's temperature, which in turn will lead to the rapid consumption of D. Depletion of D will slow down the reaction rates and diminish the generated heat leading to a temperature decrease. But at low temperatures, the accumulation of D is again possible, and the temperature will rise again. The result is a continuous oscillation of the reaction temperature and D-concentration in the reactor, with amplitudes larger as the Q-level is higher. When exceeding a certain critical Q_c value, the temperature oscillations are higher than a tolerable limit, leading to the process runaway due to the impossibility to quickly remove the heat. The study of Maria *et al.*[6] also revealed that the critical values of feeding rates $Q_c(\boldsymbol{\phi})$ depend on the operating parameter vector $\boldsymbol{\phi} = \lfloor Q, T_a, c_{D,in}, c_{P,0}, T_0 \rfloor$ around which the evaluation is made.

Predictions of critical operating conditions by various methods

Evaluation of critical feeding conditions $Q_c(\boldsymbol{\phi})$ (for a fixed D inlet concentration) starts with applying the *div*-J, by computing $\mathrm{Re}(\lambda_i(\boldsymbol{J}))$ at various reaction times for sub-critical (Fig. 1), critical (Fig. 2), and super-critical (Fig. 3) conditions. Except for the 6th eigenvalue of $\boldsymbol{J}$, which is zero all the time, corresponding to the liquid volume increase model equation (Table 1), all other eigenvalues present large variations according to the operating conditions (especially the 2nd–4th eigenvalues related to individual D reactions, and the 5th eigenvalue related to the temperature dynamics). According to the *div*-J criterion, there are no positive $\mathrm{Re}(\lambda_i(\boldsymbol{J}))$ values for inlet Q < 0.0080 L min^{-1} (Fig. 1, and Fig. 4-middle), there is an occurrence of positive values around Q = 0.0080 L min^{-1} (for the 2nd and 3rd $\boldsymbol{J}$-eigenvalues in Fig. 2, and Fig. 4-middle), and of very sharp positive peaks at super-critical conditions for Q > 0.0080 L min^{-1} (for the 2nd to 5th $\boldsymbol{J}$-eigenvalues in Fig. 3, and Fig. 4-middle). The plot of $\max_t(\max_t(\mathrm{Re}(\lambda_i(\boldsymbol{J}))))$-*vs.*-$Q$ in Fig. 4 (middle) lead to the precise prediction of the critical condition Q_c = 0.0078 L min^{-1} [div-J criterion (3)] for the nominal conditions of SBR, when using $c_{D,in}$ = 5.82 mol L^{-1}.

The same analysis has been repeated by using the SZ stability criterion (6), and computing $\mathrm{Re}(\lambda_i(\boldsymbol{J}^T\boldsymbol{J}))$ at various reaction times for sub-critical (Fig. 1), near critical (Fig. 2), and super-critical (Fig. 3) conditions. By plotting the $L_{\max}$ index *vs.* inlet Q-levels (Fig. 4-right), and by taking a small σ_j tolerance (ca. 4–5), critical condition of Q_c = 0.0083 L min^{-1} is thus estimated.

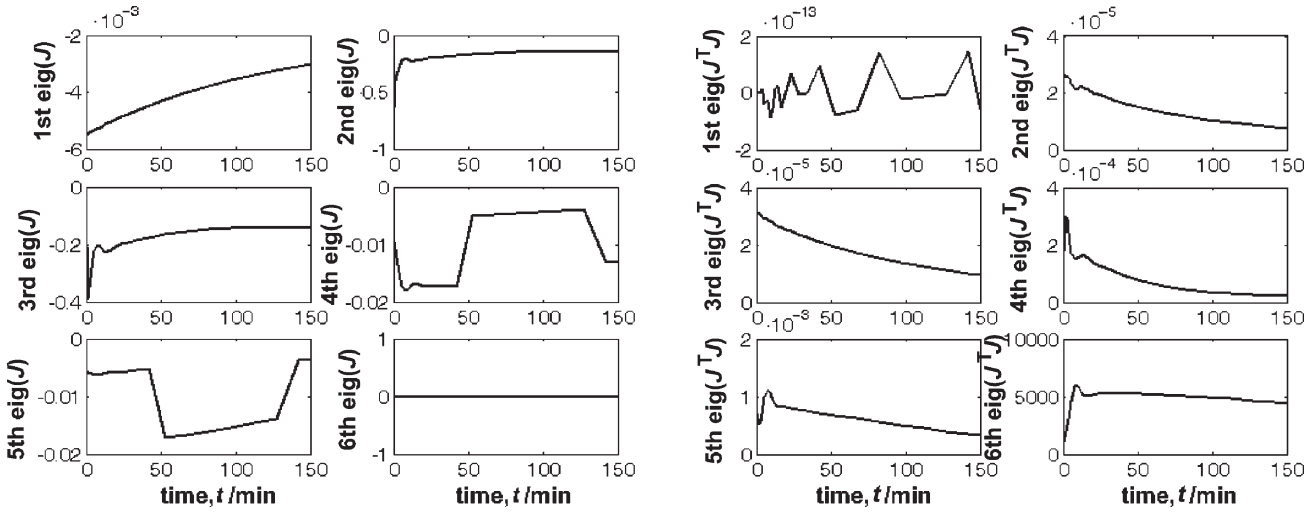

Fig. 1 – *Variation of real part of Jacobian* $\boldsymbol{J}$ *eigenvalues (left) and* $\boldsymbol{J}^T\boldsymbol{J}$ *eigenvalues (right) with the reaction time at sub-critical conditions (Q = 0.0055 L min^{-1})*

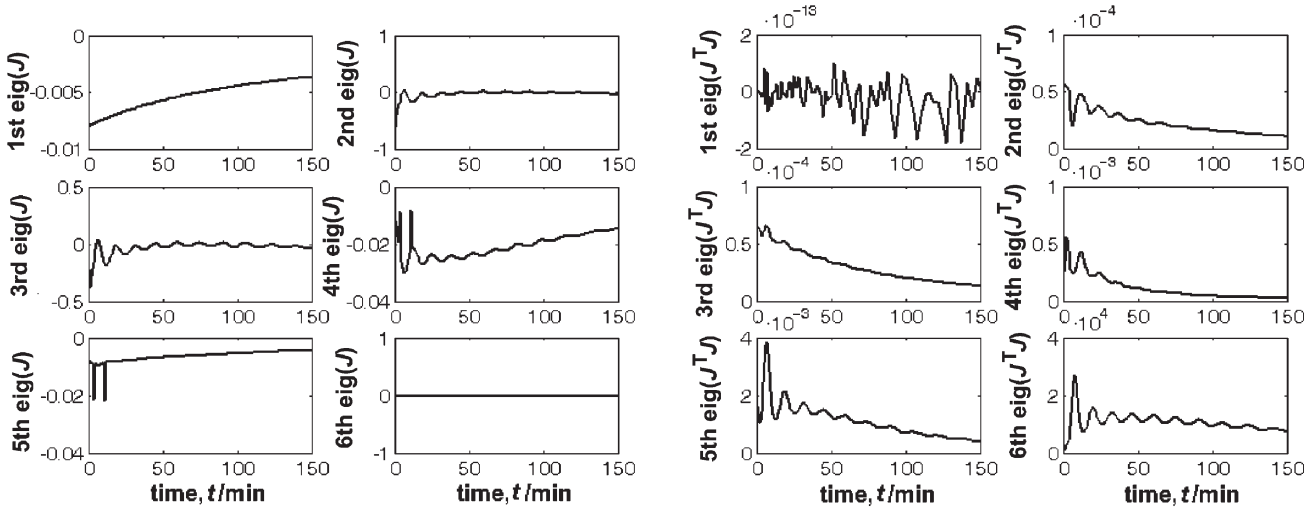

F i g . 2 – *Variation of real part of Jacobian* $\boldsymbol{J}$ *eigenvalues (left) and* $\boldsymbol{J}^T\boldsymbol{J}$ *eigenvalues (right) with the reaction time at critical conditions (*Q *= 0.0080 L min*$^{-1}$*)*

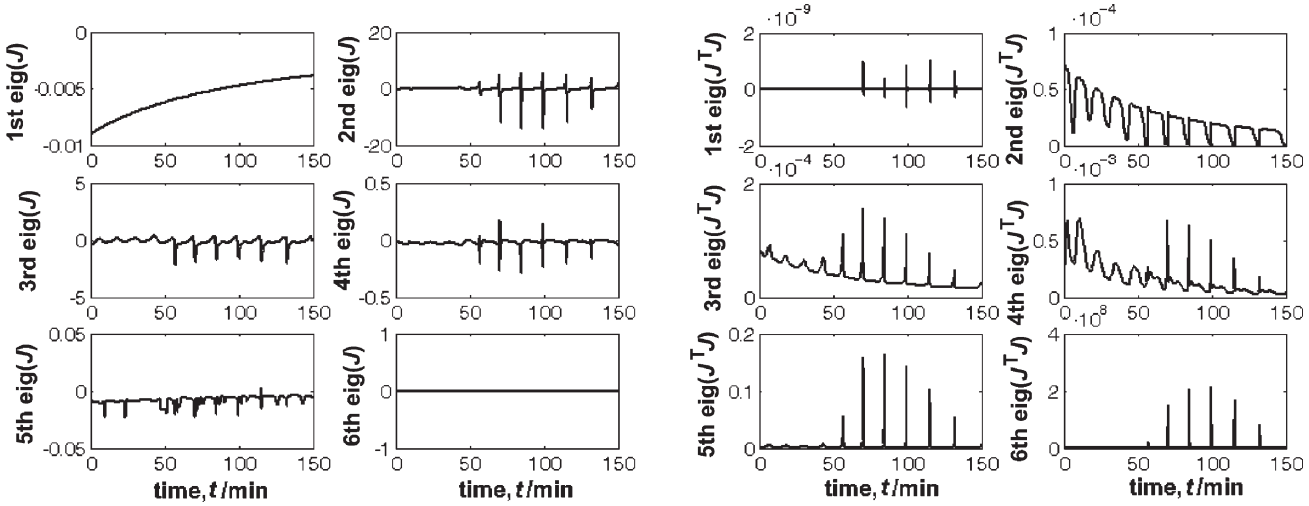

F i g . 3 – *Variation of real part of Jacobian* $\boldsymbol{J}$ *eigenvalues (left) and* $\boldsymbol{J}^T\boldsymbol{J}$ *eigenvalues (right) with the reaction time at super-critical conditions (*Q *= 0.0090 L min*$^{-1}$*)*

A quite precise evaluation of the runaway boundaries in the parametric space in sensitive regions is offered by the MV-sensitivity criterion (1). By evaluating the absolute sensitivity of the temperature maximum *vs.* the feed flow rate Q (control variable), i.e. $s(T_{\max};Q)_t$ time-dependent function at nominal conditions (Fig. 4), one can observe a sharp increase of the curve for a certain Q exceeding a critical value $Q > Q_c$. The obtained critical condition of Q_c = 0.0084 L min^{-1} is practically the same with those predicted by the *div*-SZ criterion, and higher than those predicted by the *div*-J criterion. Being more conservative, the *div*-J estimation method seems to be more suitable for early warning of any incipient instability of the process when large perturbations in operating parameters occur.

Evaluations of the derivatives required by the MV method have been performed by using the finite difference numerical method, by replacing the derivatives with finite differences of $s(T;\phi_j)_t = \Delta T(t)/\Delta\phi_j$ type, and using repeated simulations of the reactor model under various operating conditions. To keep a satisfactory evaluation accuracy of high sensitivities under severe operating conditions, small discretization steps in the parametric space have been used, i.e. $(\phi_{\max} - \phi_{\min})/n$ with n = 500, while a small time-discretization step has been set (t_f/5000) to detect all temperature peaks in the critical operating region.

The comparative evaluation of critical input Q_c has been repeated for less severe operating conditions, i.e. for a more diluted diketene feeding solution of $c_{D,in}$ = 4 mol L^{-1}. A comparative plot of results obtained with MV, *div*-J, and *div*-SZ criteria of Fig. 5 reveal quite similar predictions of critical Q_c given by MV (Q_c = 0.0128 L min^{-1}) and *div*-SZ

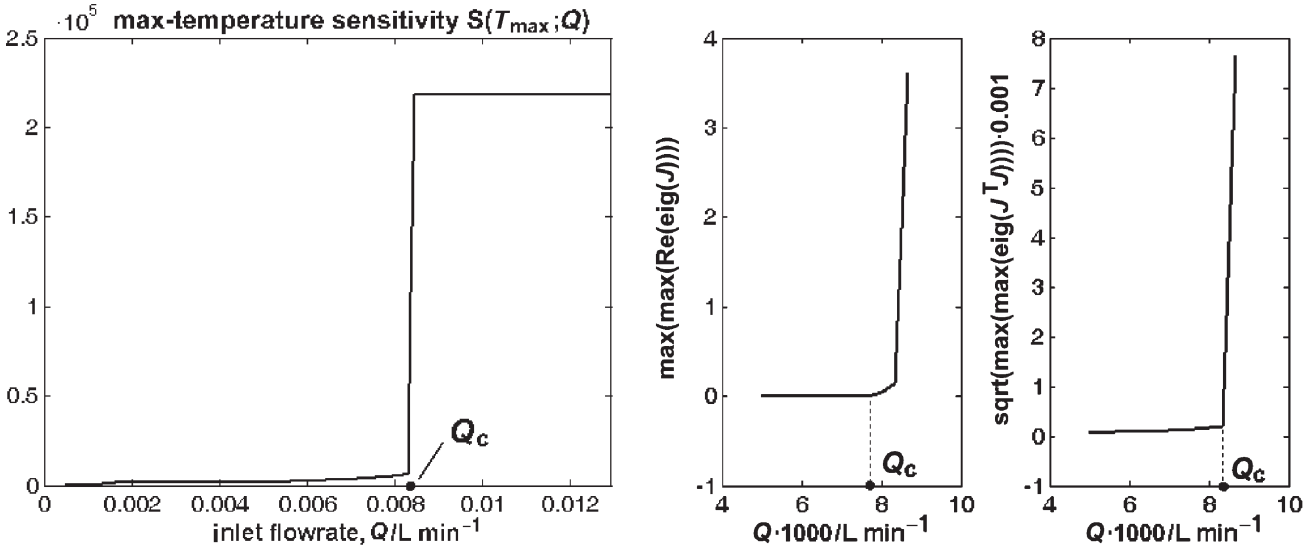

F i g . 4 – *Evaluation of the critical inlet conditions (Q_c = critical feed flow rate of diketene solution) for the semi-batch reactor at nominal conditions ($[D]_{in}$ = 5.82 mol L^{-1}) using various methods: (left) the MV sensitivity criterion; (middle) loss-of-stability div-J criterion; (right) loss-of-stability div-SZ criterion (nominal conditions correspond to 323 K, $[P]_o$ = 0.72 mol L^{-1}, batch time = 150 min)*

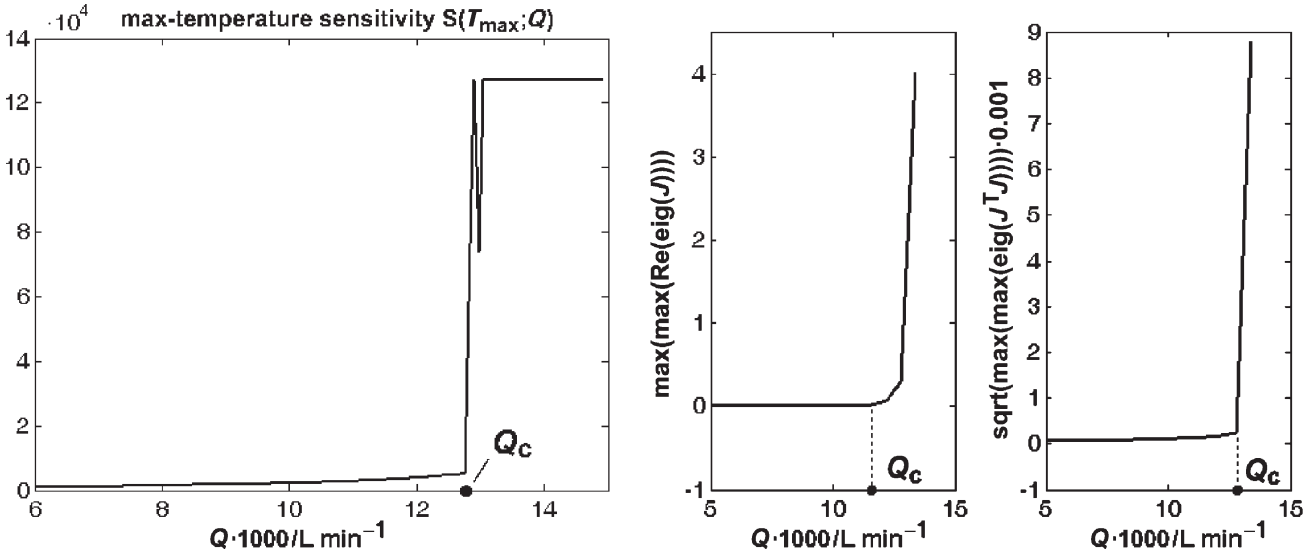

F i g . 5 – *Evaluation of the critical inlet conditions (Q_c = critical feed flow rate of diketene solution) for the semi-batch reactor at less severe inlet conditions ($[D]_{in}$ = 4.0 mol L^{-1}) using various methods: (left) the MV sensitivity criterion; (middle) loss-of-stability div-J criterion; (right) loss-of-stability div-SZ criterion (operating conditions correspond to 323 K, $[P]_o$ = 0.72 mol L^{-1}, batch time t_f = 150 min)*

(Q_c = 0.0129 L min^{-1}), and a more conservative runaway boundary predicted by the *div*-J criterion (Q_c = 0.0113 L min^{-1}). Such results confirm the recommendation to use the *div*-J analysis method for on-line detection of any incipient process instability and divergence from the reference trajectory.

The runaway analysis has been repeated by using the *div*-LY stability criterion (8), by computing LY_{max} index based on Lyapunov numbers evaluated at various reaction times. By plotting the LY_{max}-*vs.*-Q, a linear increase results for the present case study, for two checked operating conditions (Fig. 6). Such a result indicates a continuous deterioration of the system stability, but the absence of a clear 'break-point', where the plot slope might display a dramatic change, leads to the impossibility of localizing the critical conditions.

The comparative runaway analysis of the SBR continues with an evaluation of the safety boundaries under broader operating conditions, represented in separate parametric coordinates. Systematic determination of the safety limits can be made in this case for the main operating parameters $\phi = \lfloor Q, T_a, c_{D,in}, c_{P,0} \rfloor$ of the process

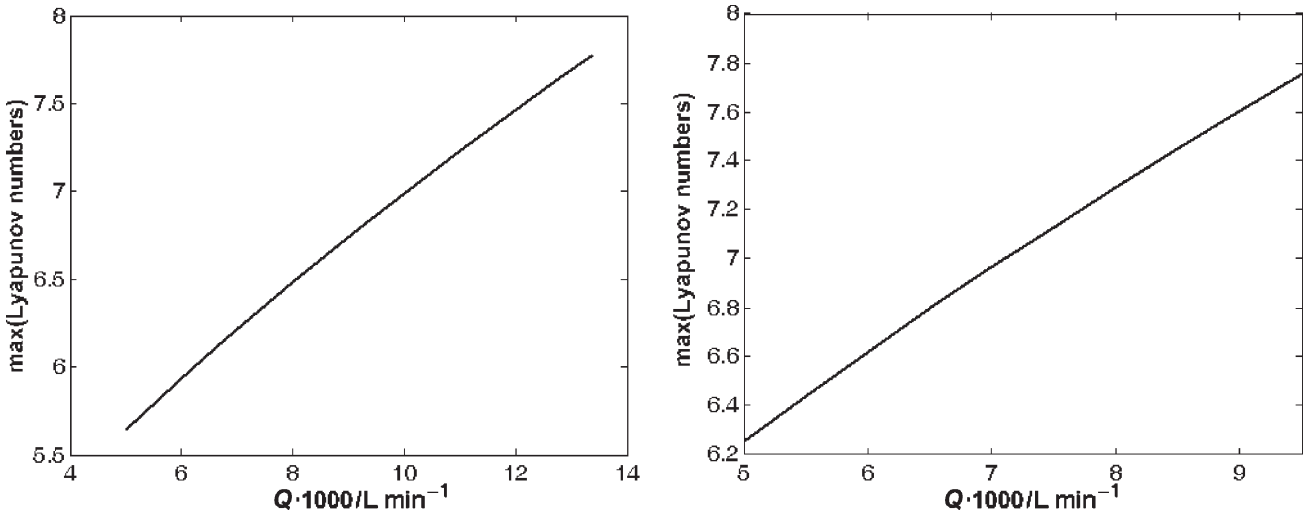

F i g . 6 – *Variation of the maximum of Lyapunov numbers (div-LY criterion) with the inlet feed flow rate of diketene solution at nominal conditions, and* $[D]_{in}$ *= 4.0 mol* L^{-1} *(left), or* $[D]_{in}$ *= 5.82 mol* L^{-1} *(right)*

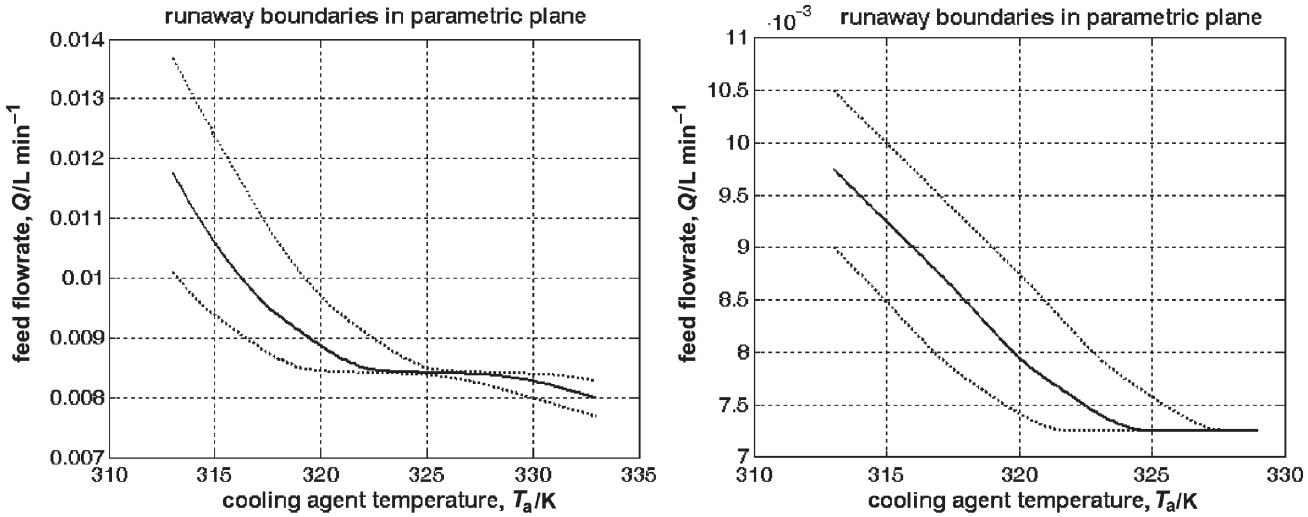

F i g . 7 – *Runaway boundaries in the [Q vs.*T_a*] plane at nominal conditions predicted by MV sensitivity method (left) and div-J criterion (right). The confidence band (---) corresponds to the random deviations in the range of* $\delta T_a = \pm 3$ *K.*

by using various sensitivity and divergence criteria.

Application of the MV criterion starts by evaluating the runaway boundaries in the $Q - T_a$ plane, by keeping nominal states for all other parameters. Thus, one evaluates the absolute sensitivity of the temperature peak $s(T_{\max}; Q)$, repeatedly done for various Q-levels under nominal conditions, and for a certain fixed value of $\phi_j = T_a$. The resulted curve (Fig. 4-left) leads to retaining the critical Q_c value corresponding to the occurrence of the maximum of $|s(T_{\max}; Q)|$. The same rule is applied for different T_a values, and the determined critical values Q_c are then represented in a $Q - T_a$ plane, thus resulting the runaway critical curve $Q_c(T_a)$. The runaway boundary (the solid curve in Fig. 7 – left) divides the $Q - T_a$ plane into two regions, corresponding to a safe (below the critical curve) or an unsafe operation (above the critical curve) of the reactor. As expected, the critical fed flow rate Q_c decreases as the operating severity increases, that is for high T_a temperatures.

The procedure is repeated by choosing another operating parameter ϕ_j (e.g. $c_{D,in}$, $c_{P,0}$, or T_0), under nominal states for all other parameters, and deriving the corresponding runaway boundaries $Q_c(\phi_j)$ in separate planes (see Fig. 8-left, and Fig. 9-left). As the obtained $Q_c(T_0)$ is roughly parallel to the T_0 abscissa, it results that the initial batch temperature has little influence on the critical Q_c over the investigated parameter domain (this plot is not presented here).

When identifying the safe/unsafe operating region in the parametric space, the parameter uncer-

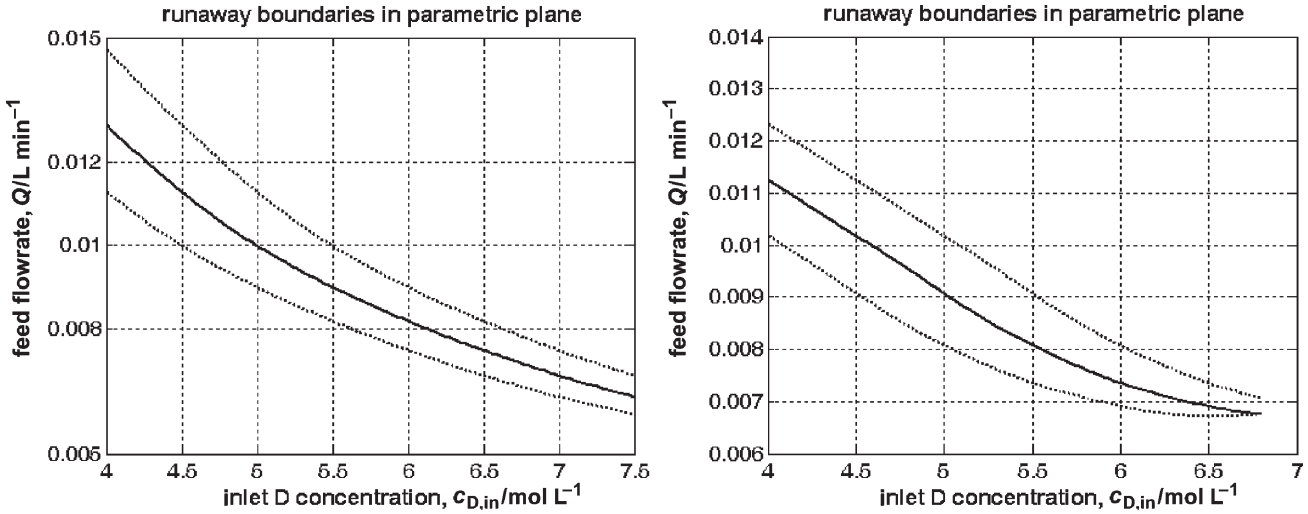

F i g . 8 – *Runaway boundaries in the [Q vs. $c_{D,in}$] plane at nominal conditions predicted by MV sensitivity method (left) and div-J criterion (right). The confidence band (- - -) corresponds to the random deviations in the range of $\delta c_{D,in} = \pm 0.5$ mol L^{-1}.*

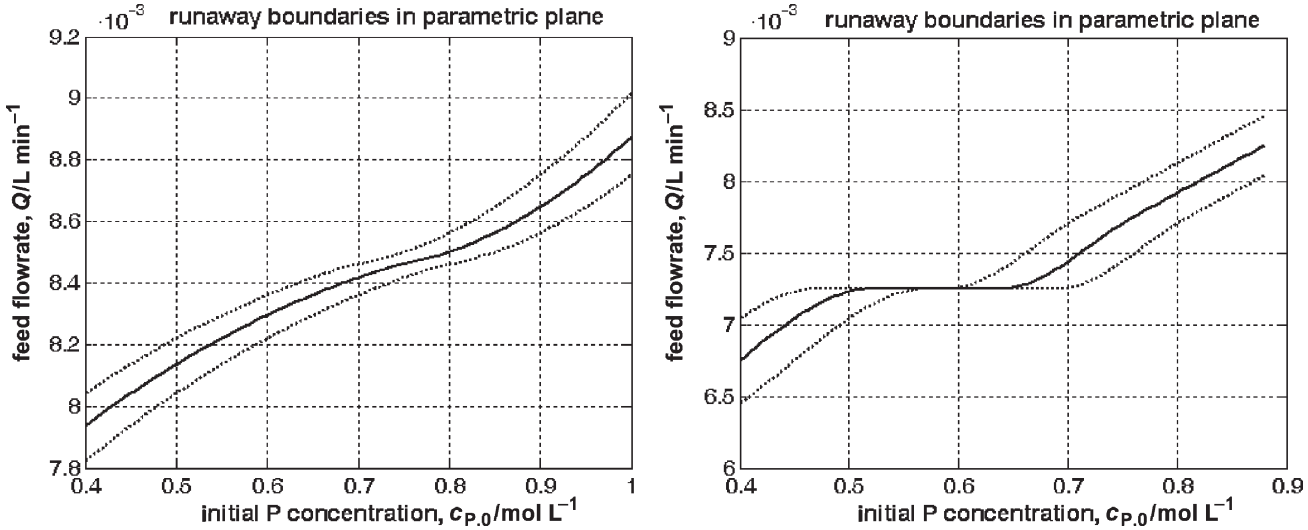

F i g . 9 – *Runaway boundaries in the [Q vs. $c_{P,0}$] plane at nominal conditions predicted by MV sensitivity method (left) and div-J criterion (right). The confidence band (- - -) corresponds to the random deviations in the range of $\delta c_{P,0} = \pm 0.05$ mol L^{-1}.*

tainty can be accounted for by evaluating the confidence region of the runaway boundaries when the set point parameters present random variations of type $\bar{\phi}_j \pm \delta\phi_j$. Consequently, when deriving $Q_c(\phi_j)$ curve, by alternatively considering the parameters at lower or upper bounds, the lower and upper bounds of the critical conditions $Q_c \pm \delta Q_c$ can thus be obtained (Figs. 7–9 left side, dotted curves). The indicated confidence band in the parametric plane corresponds to a 100 % confidence level if parameters are uniformly distributed, or to a lower confidence level for normal distributed parameters depending on the distribution characteristics (i.e. a 68 % confidence level for $\delta\phi_j = \sigma_{\phi_j}$, a 95 % confidence level for $\delta\phi_j = 2\sigma_{\phi_j}$, etc.). The approximate Q_c variance (i.e. $\sigma^2_{Q_c}$) can be estimated by using the error propagation formula for the assumed uncorrelated parameters, $\sigma^2_{Q_c} = \sum_j \left(\frac{\partial Q_c}{\partial \phi_j}\right)^2_{\bar{\phi}} \sigma^2_{\phi_j}$.[6,28] Such an uncertainty in the safety limits must be considered when determining the optimal operating policy of the SBR, usually by taking the maximum sensitivities as constraints, and keeping the solution inside the random variation region of parameters that never intersects the constraint boundaries.

The same procedure of deriving the runaway boundaries $Q_c(\phi_j)$ in separate planes can be applied by using another runaway criteria, for instance the *div*-J criterion (3). By retaining the estimated critical value Q_c under nominal conditions for T_a = 323 K (Fig. 4 centre), the same rule is re-

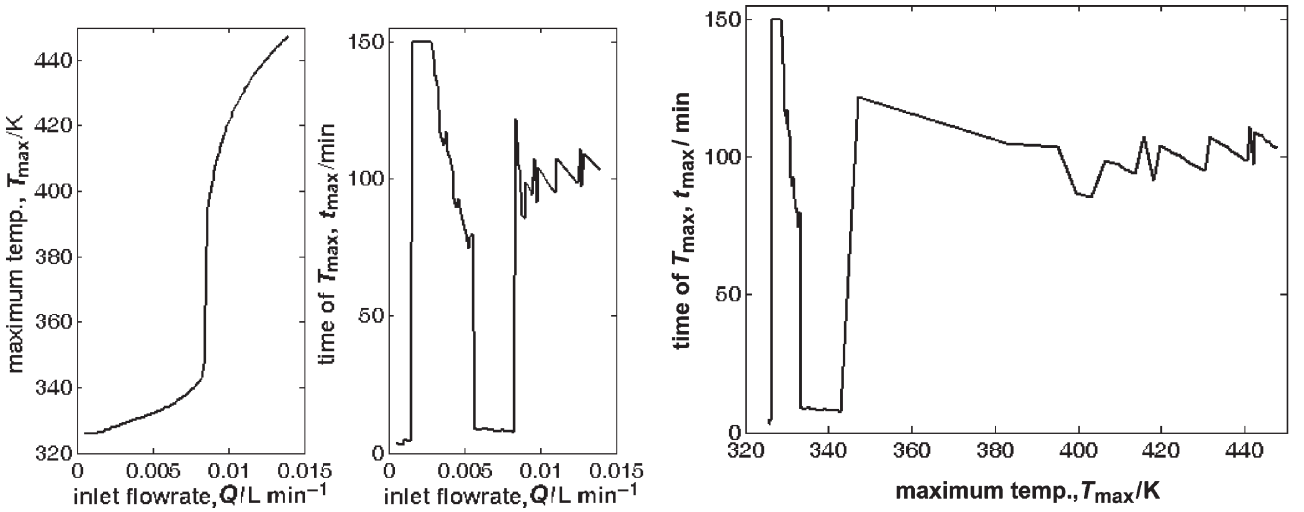

F i g . 1 0 – *Predicted maximum temperature T_{max} of the SBR (left) and time to reach the maximum temperature t_{max} (centre) as function of the inlet flow rate for θ_a = 50 °C. (right) $T_{max} - t_{max}$ curve. Values of the other parameters as in Table 1.*

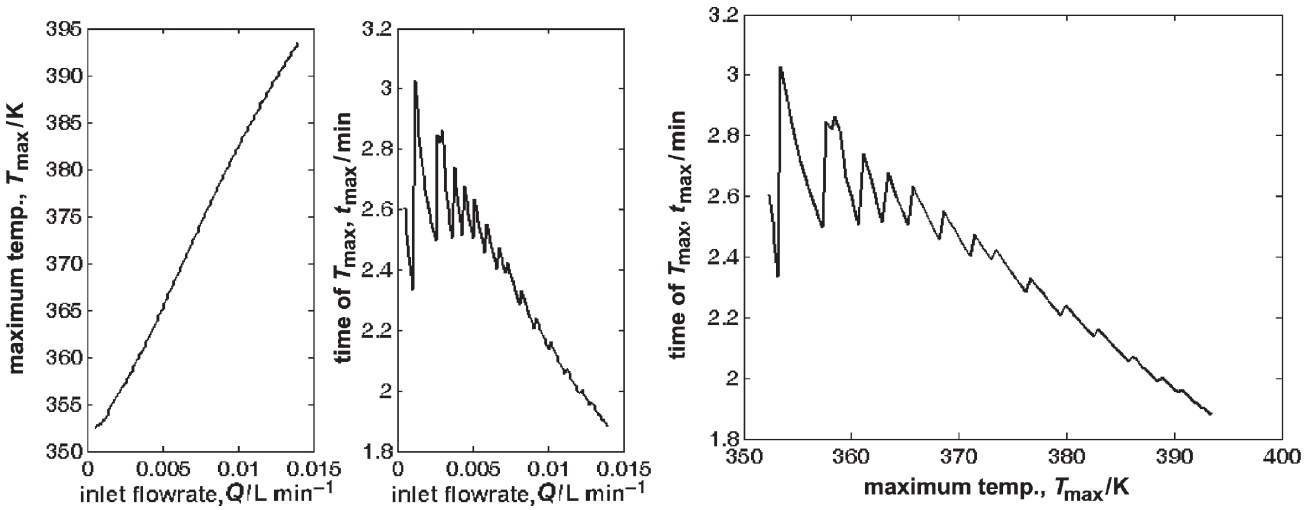

F i g . 1 1 – *Predicted maximum temperature T_{max} of the SBR (left) and time to reach the maximum temperature t_{max} (centre) as function of the inlet flow rate for θ_a = 70 °C. (right) $T_{max} - t_{max}$ curve. Values of the other parameters as in Table 1.*

peated for different T_a values, and the determined critical values Q_c are then represented in a $Q - T_a$ plane, thus resulting the critical curve $Q_c(T_a)$ (Fig. 7-right). The procedure is repeated by choosing another operating parameter ϕ_j (e.g. $c_{D,in}$, $c_{P,0}$), and the derived runaway boundaries $Q_c(\phi_j)$ are plotted in separate planes (Fig. 8-right, and Fig. 9-right, solid curves). The confidence band of the critical conditions $Q_c \pm \delta Q_c$ can be obtained on the same way as for the MV-criterion (dotted curves).

The comparison of the safety limits predicted by the MV-sensitivity and *div*-J criteria, presented in Figs. 7–9, re-confirms the tendency of some *div*-J methods to be more conservative, by predicting lower critical Q_c values and slightly wider confidence bands. Generally, the confidence region size, for a certain confidence level, depends not only on the parameter uncertainty but also on the model non-linearity and used method of estimation.

To complete the sensitivity analysis, investigation of QFS region existence is performed in the operating space. QFS area is characterized by a quasi-insensitive operation at temperatures even higher than the runaway limit. In the first step, one predicts the evolution of the maximum temperature T_{max} and of the time t_{max} to reach the maximum peak as function of one of the most influential operating parameter, that is the inlet flow rate Q. The results, plotted in Figs. 10–11 for jacket temperatures θ_a of 50 °C (nominal) and 70 °C respectively, indicate different conclusions as those obtained for single reaction case, that is: i) a continuous increase of the maximum temperature, with no peak (left plots); ii) multiple local minima in the $t_{max} - Q$ plots, at higher or lower values of t_{max}; iii) multiple local

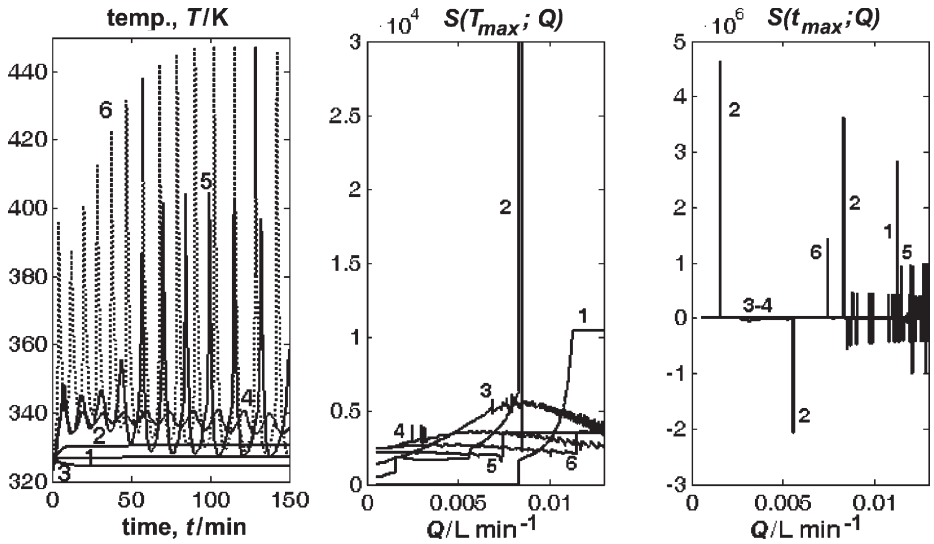

Fig. 12 – *(left) Temperature evolution during the batch time for constant fed flow rates of Q = 0.0020 L min^{-1} (1), Q = 0.0040 L min^{-1} (2), Q = 0.0060 L min^{-1} (3), Q (critical) = 0.0083 L min^{-1} (4), Q = 0.0090 L min^{-1} (5), Q = 0.0140 L min^{-1} (6). Sensitivity of the reactor maximum temperature (centre) and the time-to-maximum-temperature (right) vs. the fed flow rate for various jacket temperatures of 313 K (1), 323 K (2), 333 K (3), 343 K (4), 353 K (5), 363 K (6). Values of the other parameters as in Table 1.*

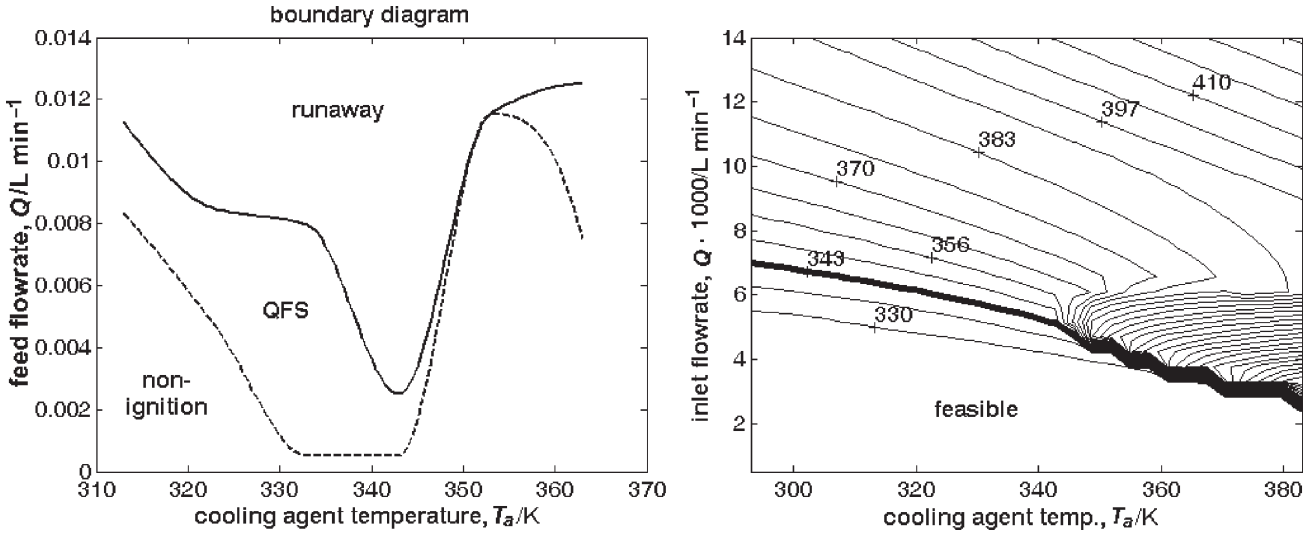

Fig. 13 – *(left) Boundary diagram for the thermal behaviour of SBR. Plots indicate the runaway boundary (—), and the inferior limit of QFS (---). (right) Maximum temperature dependence on the inlet flow rate and jacket temperature.*

minima in the $T_{max} - t_{max}$ plots. The complex successive-parallel reaction pathway, including exothermic reactions of very different enthalpy and time constants, which are successively 'ignited' at different temperatures, can explain such behaviour of the SBR. While mild and moderate operating conditions lead to a quite insensitive temperature-over-time profile (Fig. 12 left, for $Q < Q_c$ = 0.0084 L min^{-1}), higher feeding rates $Q > Q_c$ of the co-reactant inherently lead to its accumulation in the reactor. Consequently, the high-level generated heat induces an oscillatory behaviour of the temperature, which exhibits ever-growing amplitudes as the feeding rate is increasing. The successive exothermic polymerisation reactions hinder stabilisation of the temperature at super-critical conditions and a QFS operation becomes improbable.

To check the QFS location, one follows the standard procedure to build-up a boundary diagram in the $Q - T_a$ plane. Following the MV-criterion, one evaluates the $s(T_{max}; Q) - Q$ curves for different jacket temperatures T_a (Fig. 12 centre), and every time determining the critical value Q_c for runaway. Separate plot of $Q_c - T_a$ in Fig. 13 (left) splits the parametric plane in runaway and safe operating regions. Further, one evaluates the

sensitivity function of t_{max} *vs.* Q, and then plots the $s(t_{max};Q) - Q$ curves for different values of the cooling agent temperature T_a (Fig. 12, right). The result is a quite oscillatory behaviour of $s(t_{max};Q)$ in connection to the multiple local minima of the $t_{max} - Q$ plot. Consequently, application of the QFS-criterion (9) lead not to only one but to multiple starting points Q_{QFS} of the QFS region, following the characteristics of the multi-reactions from the process. If one retains the lowest Q_{QFS} value for every checked jacket temperature, the resulting boundary line of QFS region is displayed in Fig. 13 (left). It must be mentioned that such inferior limit of QFS is located in the sub-critical region, below the runaway boundary. Indeed, the operating points in the QFS area are characterized by a quite flat temperature profile, with acceptable low oscillations near the runaway limit (Fig. 12, left) and a quite fair conversion. For more severe conditions, that is for $\theta_a > 70–80$ °C, the runaway curve corresponds to higher feeding rates Q, while the non-ignition area of flat temperature profile (not presented here) is much larger.

Such a sensitivity analysis is however incomplete as long as the technological constraints are not accounted for (see Table 1, down). In the present case, higher temperature regimes and longer batch times must usually be avoided in order to prevent formation of secondary products in high amounts (such as DHA, D_n, G), while higher feeding rates are avoided in order to prevent accumulation of the co-reactant D. Experimental observations and rough calculations indicate 70 °C as being the maximum admissible temperature in the SBR, while higher temperatures lead to multiple negative effects (dangerous exothermic side-reactions, by-product formation $[DHA]_f > 0.15$ mol L^{-1}, solvent excessive vaporization and pressure increase, not included in the present model). By plotting the feasible operating region ($\theta_{max} < 70$ °C) in the same $Q - T_a$ plane (Fig. 13 right), and superposing it over the boundary diagram (Fig. 13 left), the feasible portions of the non-ignition and QFS regions are thus detected, to be of further use in locating the best SBR set-point. Such a combined analysis reveals that non-ignition region at high T_a levels is however non-feasible due to the mentioned drawbacks. Consequently, the feasibility of the problem solution is decisive for the safe operation of the SBR (even if many-times sub-optimal).

Conclusions

Despite being computationally intensive, the model-based evaluation of runaway boundaries of the operating region for an industrial reactor remains a crucial issue in all design, operation and optimal control steps. Particularly, the operation associated with inherent random parameter fluctuations around the set point, and/or operation in a higher productivity region in the vicinity of the safety limits require a precise assessment of the runaway/critical conditions. From this point of view, both *div*-methods (e.g. div-SZ), based on detection of loss of stability conditions, and parametric sensitivity (e.g. MV) methods can offer fair predictions, being quite similar and strongly connected.[8]

The method's predictions are more accurate when the checked operating region is a sensitive one, localized by preliminary model-based simulations. According to the parameter uncertainty characteristics, additional application of the same rules can provide the confidence region of the safety limits. Such information can be used together with the state variable sensitivities as constraints when deriving the optimal operating conditions of the SBR by means of a certain optimization criterion.[21,29]

As the stability analysis precedes the analysis of the system's sensitivity to perturbations,[19] a combined application of *div*- and sensitivity methods can offer better confidence in the estimated operating boundaries. Besides, both *div*- and sensitivity methods have their own value. While sensitive *div*-methods can detect early changes in the process characteristics, being recommended for on-line detection of the runaway initiation, more accurate runaway-criteria can specify the distance in the parameter space from the running/set point to the safety limits.

For a complex kinetic model, the application of sensitivity and *div*-runaway criteria is a fairly computational task. To save time, it is preferable to reduce the analysis to only the most influential parameters and initial/inlet conditions of the reactor. Also, a good choice of the method of analysis, and the correct interpretation of results are important steps in evaluating the critical conditions. While some method variants offer more conservative predictions of the critical conditions (e.g. sensitivity methods based on overall kinetics, or *div*-J method), others offer more accurate predictions (e.g. MV and *div*-SZ). Periodic determinations of the safe operating limits for an SBR exhibiting a high thermal sensitivity are also necessary when variations in the catalyst or raw-material characteristics are recorded.

An extended sensitivity analysis can reveal possible QFS regions at super-critical / severe operating conditions characterized by a quasi-stable SBR behaviour due to quasi-instantaneous reactions. Thermally insensitive regions, together with technological constraints, have to be further accounted for establishing the SBR set-point from both economic and safe operation perspective.

ACKNOWLEDGMENT

This work was supported by CNCSIS – UEFISCSU, project number PNII – IDEI 1543/2008–2011 "A nonlinear approach to conceptual design and safe operation of chemical processes".

Notations

A_r – heat exchange surface of the reactor measured inside the reactor, m^2

A – Arrhenius frequency coefficient, L mol^{-1} s^{-1}, s^{-1}

$B = \Delta T_{ad} E/(RT_0^2)$ – reaction violence index[21]

c_j – component j concentration, mol L^{-1}

c_p – specific heat capacity, J kg^{-1} K^{-1}

d_r – reactor inner diameter, m

$Da = (-\nu_A)(r_a \tau_D)/c_{A,0}$ – Damköhler number for SBR

E – activation energy, J mol^{-1}

Q – fed flow rate (liquid), L s^{-1}

$\boldsymbol{g}$ – model function vector

$\boldsymbol{G}$ – Green's function matrix

$(-\Delta H)$ – reaction enthalpy, J mol^{-1}

$\boldsymbol{J} = \partial \boldsymbol{g}/\partial \boldsymbol{x}$ – system Jacobian

k – rate constants, L mol^{-1} s^{-1}, s^{-1}

$L_{\max}$ – maximum of square root of $\boldsymbol{J}^T\boldsymbol{J}$ eigenvalues

$LY_{\max}$ – maximum of Lyapunov stability numbers

$\boldsymbol{q}$ – orthogonalized vector of $\boldsymbol{x}$

R – universal gas constant, J mol^{-1} K^{-1}

r – chemical reaction rate, mol L^{-1} s^{-1}

$s(x;\phi)$ – absolute sensitivity, $\partial x(t)/\partial \phi$

$S(x;\phi)$ – normalized sensitivity, $(\phi^*/x^*)s(x;\phi)$, or $\partial \ln(x(t))/\partial \ln(\phi)$

$St = (U A_r \tau_D)/(V \overline{\rho}\, \overline{c}_p)$ – Stanton number for SBR

t – time, s

T – thermodynamic temperature, K

$\Delta T_{ad} = (-\Delta H) c_{j,0}/(\overline{\rho}\overline{c}_p)$ – temperature rise under adiabatic conditions, K

U – overall heat transfer coefficient, W m^{-2} K^{-1}

V – liquid (reactor) volume, m^3

$\boldsymbol{x}$ – state variable vector

Greeks

α_i – Lyapunov stability numbers

Δ – finite difference

δ – Kronecker delta function, or small perturbation

$\delta \boldsymbol{x}$ – perturbation of the fiducial trajectory

ϕ – operating parameter

λ_j – eigenvalues of a matrix

$\tilde{\lambda}_j$ – Lyapunov exponents

ν_j – stoichiometric coefficient of species j

ρ – liquid phase density, kg m^{-3}

σ – standard deviation, or relative sensitivity tolerance

τ – time constant, s

τ_D – time of addition of co-reactant D, s

θ – temperature, °C

Index

a – cooling agent

ad – adiabatic

c – critical

f – final

in – inlet

max – maximum

min – minimum

o – initial

$\overline{\bullet}$ – average value

Abbreviations

D – diketene

DHA – dehydroacetic acid

G – secondary product

GM – geometry-based methods

MV – Morbidelli-Varma criterion

P – pyrrole

PAA – 2-acetoacetyl pyrrole

PSA – sensitivity-based methods

Py – pyridine

Re(·) – real part

SBA – stretching-based method

SBR – semi-batch reactor

SZ – Strozzi & Zaldivar

Trace(·) – trace of a matrix

References

1. *Grewer, T.*, Thermal hazards of chemical reactions, Elsevier, Amsterdam, 1994.
2. *Varma, A., Morbidelli, M., Wu, H.*, Parametric sensitivity in chemical systems, Cambridge University Press, Cambridge (MS), 1999.
3. *Stoessel, F.,* Thermal safety of chemical processes. Risk assessment and process design, Wiley-VCH, Weinheim, 2008.
4. *Stefan, D. N., Maria, G.,* Revista de Chimie **60** (2009) 949.
5. *Maria, G., Stefan, D. N.,* Jl. Loss Prevention in the Process Industries **23** (2010) 112.
6. *Maria, G., Dan, A., Stefan, D. N.,* Chemical and Biochemical Engineering Quarterly **24** (2010) 265.
7. *Adrover, A., Creta, F., Giona, M., Valorani, M.,* Chemical Engineering Science **62** (2007) 1171.
8. *Vajda, S., Rabitz, H.,* Chemical Engineering Science **47** (1992) 1063.
9. *Zaldıvar, J. M., Cano, J., Alos, M. A., Sempere, J., Nomen, R., Lister, D., Maschio, G., Obertopp, T., Gilles, E. D., Bosch, J., Strozzi, F.,* Journal of Loss Prevention in the Process Industries **16** (2003) 187.

10. *Strozzi, F., Zaldivar, J. M.,* Chemical Engineering Science **49** (1994) 2681.
11. *Strozzi, F., Zaldıvar, J. M., Kronberg, A. E., Westerterp, K. R.,* AIChE Journal **45** (1999) 2429.
12. *Alos, M. A., Nomen, R., Sempere, J. M., Strozzi, F., Zaldıvar, J. M.,* Chemical Engineering and Processing **37** (1998) 405.
13. *Westerterp, K. R., Molga, E. J.,* Ind. Eng. Chem. Res. **43** (2004) 4585.
14. *Seider, W. D., Brengel, D., Provost, A.,* Ind. Eng. Chem. Res. **29** (1990) 805.
15. *Bonvin, D.,* J. Proc. Cont. **8** (1998) 355.
16. *Abel, O., Marquardt, W.,* Journal of Process Control **13** (2003) 703.
17. *Ruppen, D., Bonvin, D., Rippin, D. W. T.,* Computers & Chemical Engineering **22** (1997) 185.
18. *Zwillinger, D., Krantz, S. G., Rosen, K. H.,* Standard mathematical tables and formulae, CRC Press, Boca Raton, 1996, pp. 705.
19. *Hedges Jr., R. M., Rabitz, H.*, J. Chem. Phys. **82** (1985) 3674.
20. *Char, B. W., Geddes, K. O., Gonnet, G. H., Leong, B. L., Monagan, M. B., Watt, S. M.,* MAPLE 5 Library Reference Manual, Springer-Verlag, Heidelberg, 1991.
21. *Chen, M. S. K., Erickson, L. E., Fan, L.,* Ind. Eng. Chem. Process Des. Develop. **9** (1970) 514.
22. *Bosch, J., Kerr, D. C., Snee, T. J., Strozzi, F., Zaldıvar, J. M.,* Industrial & Engineering Chemistry Research **43** (2004) 7019.
23. *Zaldıvar, J. M., Strozzi, F., Bosch, J.,* AIChE Journal **51** (2005) 678.
24. Zaldıvar, J. M., Strozzi, F., Chemical Engineering Research and Design **88** (2010) 320.
25. *Nakano, K., Kosaka, N., Hiyama, T., Nozaki, K.*, Dalton Trans. (2003) 4039.
26. *Martínez, E.*, Batch-to-batch optimization of batch processes using the STATSIMPLEX search method, 2nd Mercosur Congress on Chemical Engineering, Costa Verde (Rio de Janeiro), Brasil, 2005, paper #20.
27. *Froment, G. F., Bischoff, K. B.,* Chemical reactor analysis and design, Wiley, New York, 1990.
28. *Park, S. W., Himmelblau, D. M.,* AIChE Jl. **26** (1980) 168.
29. *Seinfeld, J., McBride, W. L.*, Ind. Eng. Chem. Process Des. Develop. **9** (1970) 53.
30. *Alos, M. A., Strozzi, F., Zaldivar, J. M.,* Chemical Engineering Science **51** (1996) 3089.
31. *Maria, G., Stefan, D. N.,* Chemical Papers **64** (2010) 450.
32. *Steensma, M., Westerterp, K. R.,* Ind. Eng. Chem. Res. **29** (1990) 1259.
33. *Steensma, M., Westerterp, K. R.*, Chem. Eng. Technol. **14** (1991) 367.